



EARTHQUAKE RESPONSE FOR STRATIFIED DEPOSITS COMPOSED OF CLAY AND SAND LAYER BY ON LINE PSEUDO-DYNAMIC RESPONSE TEST

**Norimasa YOSHIMOTO¹, Masayuki HYODO², Naoki TAKAHASHI³, Yoichi YAMAMOTO⁴ and
Shinya KIMURA⁵**

SUMMARY

In this study, on-line pseudo-dynamic response tests were conducted on the earthquake response characteristics of alternating layers of clay and sand to precisely investigate the effects of the degree of consolidation of clay on the vibration properties of the alternating layers. It was concluded that: (1) The time-history deformation characteristics of clay varied depending on its degree of consolidation and stress history. The difference affected the degree of liquefaction of overlying sand layers, and the strain generated in the overlying layers was the smallest for the under-consolidated clay, followed by normally consolidated clay and over consolidated clay in ascending order. (2) Tests in which the depth of a clay layer was changed showed that there was a marked development of strain just beneath the clay layer. (3) Cumulative energy loss was larger in clay than in sand, and was largest in the under-consolidated clay, followed by normally consolidated and over-consolidated clays, in that order.

INTRODUCTION

The Michoacan Earthquake, which occurred in Mexico in 1985 (Mendoza and Auvinet, 1988), and the Loma Prieta Earthquake, which occurred in 1989 in the US along the San Francisco Bay (Yasuhara, 1999; JSCE Earthquake Engineering Committee, 1990a-c), are typical examples of earthquakes in which soft clayey layers amplified the ground motion and worsened the overall degree of damage. During the latter earthquake, the recorded accelerations on soft ground layers were two to three times larger than those on hard ground (JSCE Earthquake Engineering Committee, 1990c, JGS, 1994). On the other hand, there have been cases in which soft layers acted like dampers and reduced damage, an example of which is the small amount of damage to the Imperial Hotel in Tokyo during the Great Kanto Earthquake

¹ Yamaguchi University, Japan, nyoshi@yamaguchi-u.ac.jp

² Yamaguchi University, Japan, hyodo@yamaguchi-u.ac.jp

³ Sumitomo Mitsui Construction Co., Ltd, Japan, tnaoki@smcon.co.jp

⁴ Sumitomo Mitsui Construction Co., Ltd, Japan, yoichiyamamoto@smcon.co.jp

⁵ Japan Engineering Consultants Co., Ltd, Japan

(Fukutake, 2001). Frank Lloyd Wright designed and constructed the foundation of the hotel to act as a floating raft using the damping effects of the soft ground (Akashi, 1972; Futagawa, 1980). Since soft clay ground layers both amplify and attenuate ground motion, the effects of the nonlinearity of their earthquake response characteristics on the ground surface needs to be understood.

Response characteristics of the ground vary in complicated ways, depending on the layer thickness, elastic wave velocity, damping coefficient, density, and the frequency characteristics of the input ground motions. Furthermore, in soft ground the nonlinearity of clay may strongly influence the response characteristics of the ground during earthquakes. Although effective stress analysis is generally applied to saturated sandy layers, clay layers have been considered to be elastic bodies. However, it is important to consider the nonlinear characteristics of clay to evaluate ground response characteristics of the ground during an earthquake. We have developed an on-line dynamic testing system to investigate the earthquake response of stratified ground. In this method, a dynamic response analysis and a pseudo-dynamic loading test that experimentally determines the restoring force of a material are combined by a computer into an on-line data processing system. This system was used to investigate the earthquake response of stratified ground that includes a clay layer. In these analysis, parameters for the strata, the thickness of the layers, and the depth of the clay layer were varied, to examine the influence of these parameters on the amplification of earthquake movement and the liquefaction of a sand layer.

ON-LINE PSEUDO-DYNAMIC RESPONSE TEST PROCEDURE

Concepts of the on-line pseudo-dynamic response test

The principles of the on-line pseudo-dynamic response test are shown in Figure 1. This system, which was developed by Kusakabe et al. (1990), involves the following algorithm. First, the ground to be analyzed is converted into a lumped mass model into which earthquake motion is input at the base. Next, the vibration equation of the mass system is solved using a computer to determine the displacement response of each mass. The shear strain that is equivalent to the resultant displacement is applied to a specimen under computer control. The corresponding restoring force that is then automatically monitored is used to calculate the displacement response for the next step. This process is repeated for as long as the earthquake motion continues in order to directly determine the constantly changing nonlinear restoring force of the ground from the element tests. The element experiments were conducted using a simple shear test, developed by Kusakabe et al. (1999), Figures 2(a) and 2(b). A harmonic-gear AC servo-motor provided high precision for displacement control. Shear strain was measured by a non-contact type displacement transducer, while the total axial stress and the shear stress on the specimen were measured using a two-directional load cell. The effective horizontal confining pressure on the specimen was measured by a differential pressure transducer. A 14-bit A/D converter was used for data acquisition.

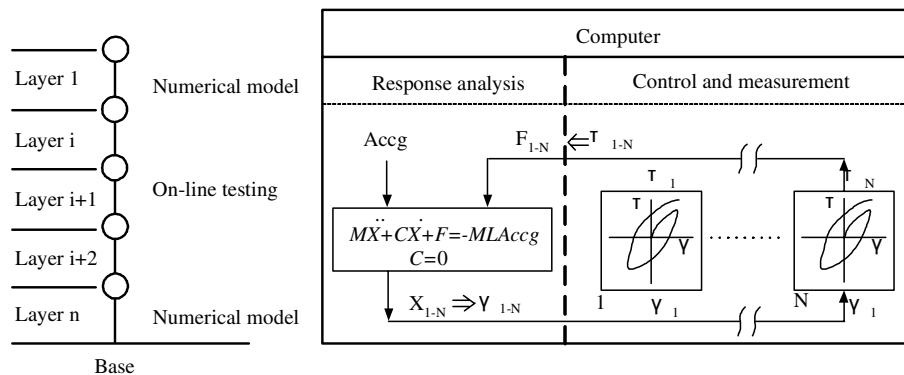


Figure 1 Conceptual diagram of on-line earthquake response test

Since testing the entire ground profile, which consisted of a number of layers, would make the system both expensive and complicated, only the ground elements that were likely to be prone to liquefaction and deformation were tested to analyse the restoring force. The restoring forces of other sections were estimated numerically using modified Ramberg-Osgood models (Desai et al., 1985).

$$M\ddot{X} + C\dot{X} + F = -MLA_{ccg} \quad (1)$$

$$C = 0 \quad (2)$$

Where:

M is the mass matrix; C is the damping matrix; F is the restoring force vector; L is a unit vector; Accg is the input acceleration; and X is the displacement vector. The linear acceleration method was used for the initial numerical integration, and the central difference method was then used for subsequent steps (Shibata, 1981).

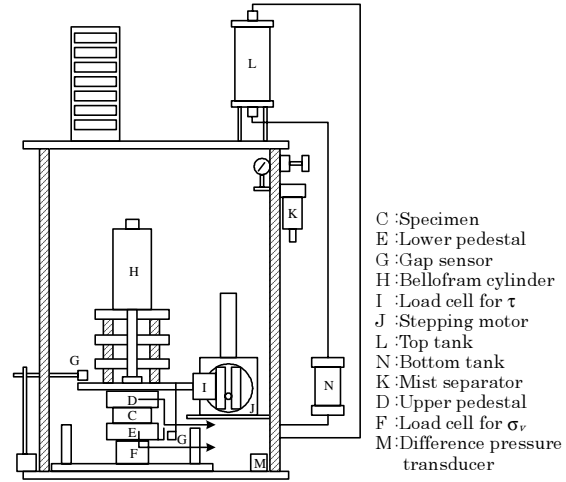
ON-LINE PSEUDO-DYNAMIC RESPONSE TEST METHODS

(1) Ground model

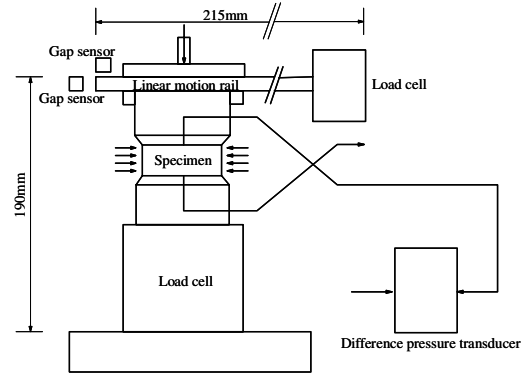
As shown in Figure 3, the model of the ground was prepared by assuming a horizontally stratified ground of a depth of 18m and dividing the ground into six layers, each of which was replaced by a one-dimensional mass system model. The restoring forces of layers were determined by measuring the forces in element experiments for L2 to L4 (GL-3m to GL-12m) and using modified Ramberg-Osgood models for the other layers. Layers L2 to L4 were chosen as clay or liquefiable sand layers with relative density $Dr = 50\%$. The configuration of the layers was varied as shown in Table 1. L1 was a liquefiable sand layer with $Dr = 50\%$ above the groundwater level and L5 to L6 were sand layers with $Dr = 80\%$, which were not prone to liquefaction.

(2) Element experiments

Element tests were carried out using three sets of simple shear apparatus (Kusakabe et al., 1999). Shearing was carried out under undrained conditions with zero vertical, lateral and volumetric strains. The loads were applied using stepping motors with a maximum rate of strain (0.3%/min.) due to equipment limitations. The soils used for the element experiments were Onoda clay, a marine clay sampled in Onoda City, Yamaguchi Prefecture, ($G_s = 2.601$, $W_L = 80.9\%$, $W_p = 34.9$, $I_p = 46.0$), and Toyoura Sand ($G_s = 2.643$, $e_{max} = 0.973$, $e_{min} = 0.635$). Reconstituted clay specimens were prepared by thoroughly mixing a slurry to twice the liquid limit and pouring it into consolidation cells. A vertical consolidation pressure of $\sigma_{vc} = 10$ kPa was applied for one day and then 20 kPa for a further day followed by a pressure of $\sigma_{vc} = 50$ kPa for two weeks. Samples were assembled in the simple shear apparatus with porous stones on the



(a) The system diagram for simple shear apparatus



(b) Expanded diagram for loading system and specimen
Figure 2 Simple shear testing system

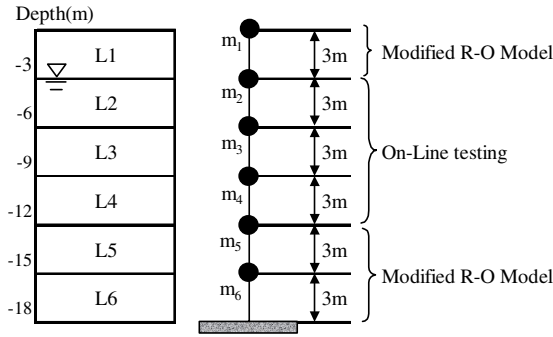


Figure 3 Ground model

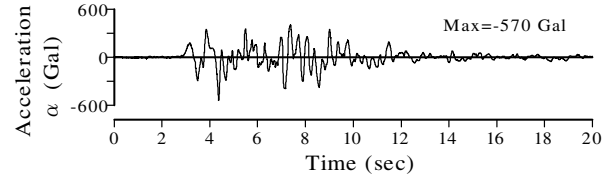


Figure 4 Input base motion

Table 1 Test Configurations

Layer	TEST							
	SSS	SSC _{U50}	SSC	SSC _{OCR5}	SCS	CSS	CCS	CCC
L1	Sand ($D_r = 50\%$)							
L2	Sand	Sand	Sand	Sand	Sand	Clay	Clay	Clay
L3	Sand	Sand	Sand	Sand	Clay	Sand	Clay	Clay
L4	Sand	Clay	Clay	Clay	Sand	Sand	Sand	Clay
L5	Sand ($D_r = 80\%$)							
L6	Sand ($D_r = 80\%$)							

Table 2 Analytical Parameters

Layer	Thickness (m)	Unit Weight γ (kN/m ³)	Shear strength τ_f (kPa)	Shear modulus G_0 (MPa)	α	β
L1	3	19.1	13.9	48.7	2.45	2.29
L2	3	19.1	On-line	On-line	-	-
L3	3	19.1	On-line	On-line	-	-
L4	3	19.1	On-line	On-line	-	-
L5	3	19.6	128.5	152	2.45	2.29
L6	3	19.6	159.8	164.7	2.45	2.29

base and top platens and a latex membrane around the outside. Three different consolidation regimes were imposed on the clay samples used in this apparatus. Normally consolidated samples were produced by applying a negative pore water pressure to the top platen and allowing drainage for 24 hours. 50% under-consolidated specimens were prepared using a similar technique but stopping the drainage when the top platen displacement reached 50% of the normally consolidated value. Finally OCR=5 samples were first subjected to consolidation and swelling regimes in an oedometer cell and then mounted in the simple shear apparatus for on-line testing. In this case the same vertical stress σ_v as in the oedometer was imposed and making the assumption that K_0 in the oedometer was 0.4, a lateral pressure of $0.4\sigma_v$ was applied. The sand specimens were prepared by pluviating Toyoura sand in water to a pre-determined relative density. The dimensions of the specimens were approximately 60 mm diameter and 40 mm height. To reduce the consolidation period the height of the clay specimens only were reduced to 20 mm. Anisotropic consolidation with a coefficient of earth pressure at rest $K_0 = 0.4$, was achieved by applying σ_h' and σ_v' in stages up to the predetermined values.

(3) Experimental and analytical conditions

The on-line pseudo-dynamic response tests were conducted for layers L2 to L4, and the restoring forces were determined for varying degrees of consolidation of the clay layers, layer thicknesses, and order of layers (Table 1). The test notation in the table indicates the soil layering. "SSC" for example, means that L2 to L4 were sand, sand, and clay, respectively. For cases in which L4 was clay, SSC_{U50} denotes non-consolidated clay with a 50% degree of consolidation and SSC_{OCR5} denotes clay with an overconsolidation ratio of 5. All other clay layers were normally consolidated. The analytical parameters chosen for the modified Ramberg-Osgood models are shown in Table 2. The earthquake input waves were those observed at location PI-79mNS (maximum acceleration of 570 Gal), at a depth of 79m on Kobe Port Island during the 1995 Hyogo-ken Nanbu Earthquake (Figure 4).

EFFECTS OF THE DEGREE OF CONSOLIDATION OF CLAY LAYERS ON EARTHQUAKE RESPONSE CHARACTERISTICS

(1) Stress-strain relationships and effective stress paths

Figure 5 shows the relationships between shear stress τ and shear strain γ for layers L2 to L4. In test SSS, in which all layers were sand, the shear stress values for layers L2 and L3 were largest at Peak A, which is shown with a circle in the figure, and reduced thereafter. Peak A was about 3 to 4 seconds after the start of stress input. At this point, the strain was 0.67% in L2 and was 1.4% in L3. The excess pore water pressure ratios, u/σ_v' , were 0.36 and 0.34, respectively. The figure shows that reduction in shear stress was accompanied by little change in strain amplitude. After Peak A, the reduction in stiffness progressed, and liquefaction occurred causing the strain in these layers to jump and the shear stress to drop to almost zero. On the other hand, L4 developed a strain of approximately 2%, softened, but did not reach liquefaction. When layer L4 was clay, the stiffness increased in the order of non-consolidated, normally consolidated, and over-consolidated; and the strains which were stiffness dependent, decreased in this order. The figure shows that the time-history loops were less circular for more consolidated clay, showing that the non-linear time dependant deformation characteristics of clay vary depending on its stiffness. Unlike sand, clay did not show drastic drops in stiffness even at large strains, but retained a certain degree of stiffness and did not liquefy. As for SSS, the sand layers, L2 and L3, either liquefied or almost liquefied. The development of the strain in these layers depended on the degree of consolidation of the underlying clay, and was higher in more consolidated clay; and thus the more consolidated the underlying clay the more severe the liquefaction of L2 and L3. This shows that the degree of hysteresis and magnitude of stiffness seen in the time-history deformation characteristics of a clay layer determine the degree of liquefaction of upper sand layers.

Figure 6 shows the effective stress paths for layers L2 to L4. For sand layers, the figure also shows the phase transformation line (PTL) for Toyoura sand which represents the stress ratio at which loose sand samples change from compressive to dilative behaviour (Alarcon-Guzman et al., 1988). This was derived from the results of off-line monotonic undrained tests. In all cases, layers L2 and L3 showed rapid deformation and liquefied or almost liquefied immediately after the stress ratio exceeded the phase transformation line. In sandy L4, the effective stress decreased almost reaching the phase transformation line but the mean principal effective stress did not become zero but instead reached a constant value of approximately 50% of the initial effective confining pressure. In the case of the under-consolidated clay in Layer 4 in the SSC_{U50} test a pore pressure equal to 50% of the consolidation pressure existed at the start of the test as can be seen on the effective stress path in Figure 6. The reduction in effective stress in the clay depended on the degree of consolidation. In the over-consolidated clay, the drop was only 10% of the initial confining pressure while the drop was 90% in the under-consolidated clay. Therefore, an under-consolidated clay would be more prone to reductions in effective stress although the degree is not as excessive as in sand which suffers liquefaction.

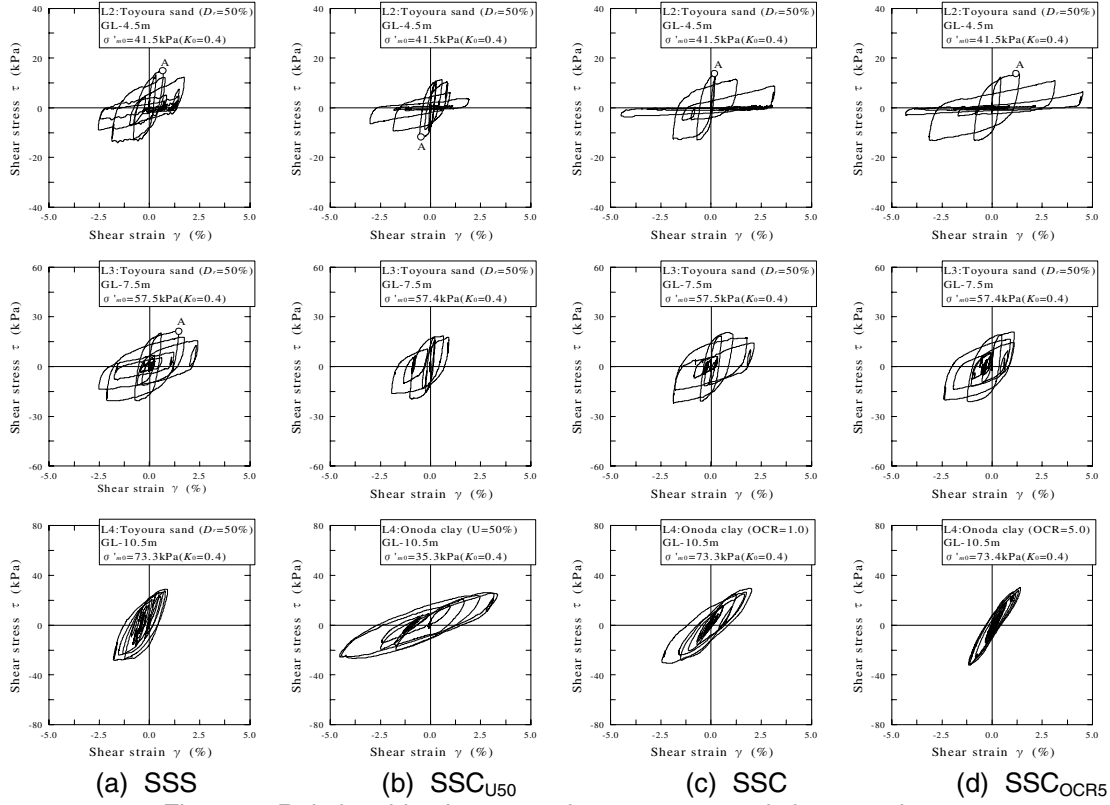


Figure 5 Relationships between shear stress τ and shear strain γ

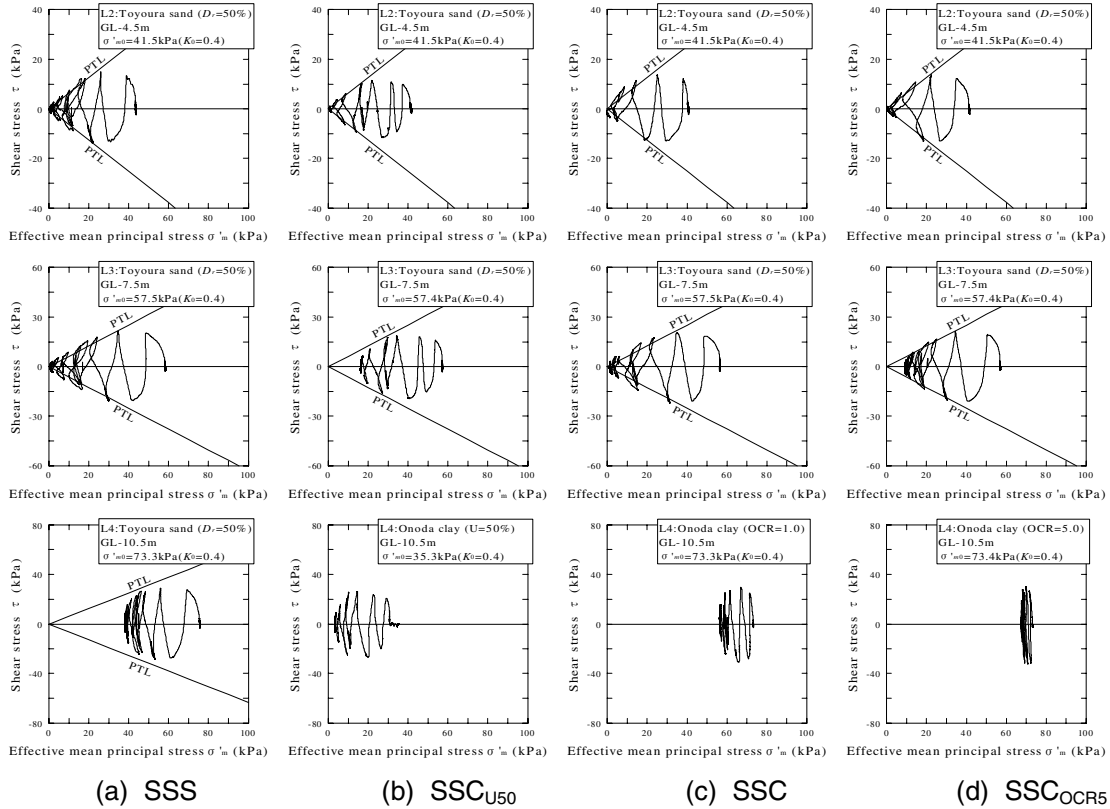
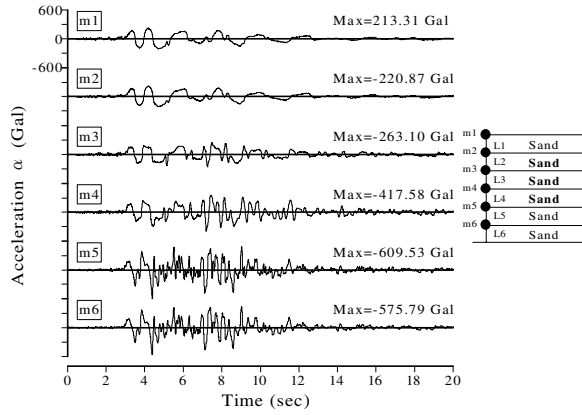
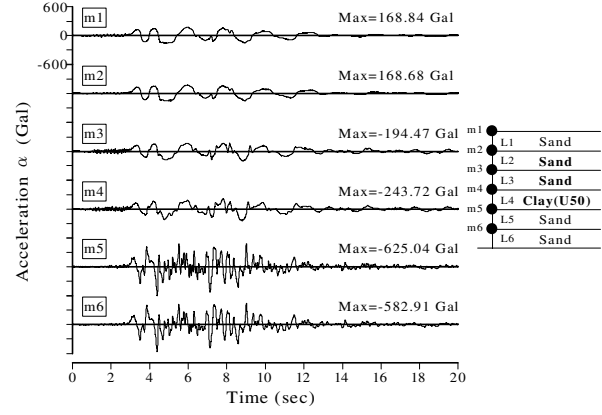


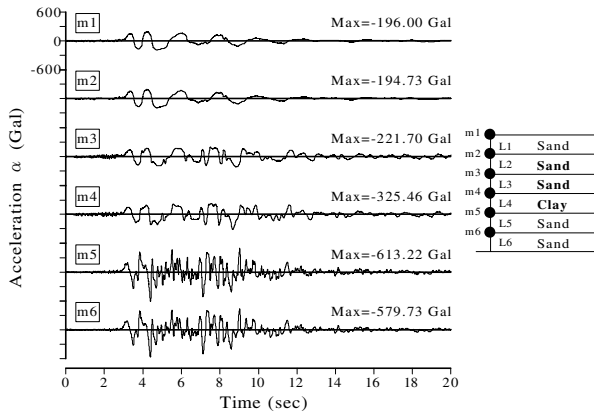
Figure 6 Effective stress paths



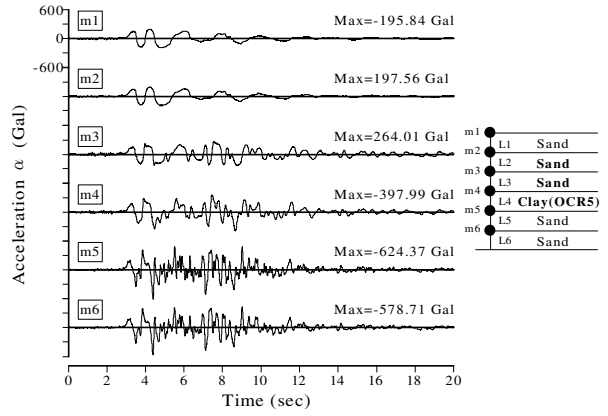
(a) SSS



(b) SSC_{U50}



(c) SSC



(d) SSC_{OCR5}

Figure 7 Acceleration time histories

(2) Acceleration time-history

Figure 7 shows the time-history of the acceleration α for masses m1 to m6. For m2, the acceleration was attenuated in all cases, causing the waveforms to have longer periods. This tendency was also observed at mass point m1. Such attenuation was caused by reductions in shear modulus of layers L2 and L3 during liquefaction, which inhibited the propagation of the earthquake motion to the upper layers. On the other hand, for m4, the long period components were more predominant for the clay layers than for the sand layer in the SSS configuration. This tendency was especially marked in the non-consolidated clay, suggesting that the clay layers filtered out the high-frequency components. Since clay layers are not prone to large reductions in stiffness leading to liquefaction, such an effect of clay was probably attributable to the plastic hysteretic deformation of the ground consuming large amounts of energy.

EFFECTS OF LAYER CONFIGURATION AND THE THICKNESS OF CLAY LAYERS ON THE EARTHQUAKE RESPONSE CHARACTERISTICS

(1) Stress-strain relationships and effective stress paths

Figure 8 shows the relationship between shear stress and shear strain for layers L2 to L4 for SCS, CSS, CCS, and CCC configurations. The sand layer L2 of the SCS configuration, in which a clay layer was between two sand layers, showed a development of strain along with a reduction in stiffness and liquefaction. However layer L4, which was just below the clay layer, also showed markedly larger strain development than the strain development shown in Figure 4 for SSS, the sand only configuration. Layer L3 in CSS and layer L4 in CCS also showed a similar tendency. Thus in sand layers underlying clay there was a relatively large hysteresis and loss of energy. The effective stress paths of these layers (Figure 9) showed sharp drops of effective stress, and a rapid increase in deformation immediately after the stress ratio exceeded the phase transformation line and the layers liquefied or almost liquefied. In CCC, which had clay layers L2 to L4, all layers showed strains of over 2% but no drastic drops in stiffness leading to liquefaction. Their effective stress dropped by only 30 to 40% of the initial confining pressure when an equilibrium was reached and no further changes in effective stress occurred.

(2) Acceleration time-history

Figure 10 shows the acceleration time history for masses m1 to m6 in the SCS, CSS, CCS, and CCC configurations. The waveform for mass m2 in the SCS test in which L2 liquefied, showed an increase in period and attenuation caused by the vibration, but no such attenuation was seen for masses m3 and m4 probably because L4 did not liquefy but retained a degree of stiffness. For the CSS test, the waveform for mass m2 contained a relatively large quantity of short period components although layer L3 liquefied. This was likely to be because short period components were relatively predominant in the waveform at mass point m4 and increased the higher frequency response of the layer, which then affected the earthquake response of the upper layers. In the CCS test, the response of clay layers m2 and m3 was attenuated along with the vibration. Since normally consolidated clay does not normally attenuate vibrations in the same way as that observed during liquefaction of sandy layers, the attenuation in the clay layers can be attributed to L4, which liquefied and inhibited the propagation of shear waves to the upper layers. Finally, in CCC, the long period components of the waveforms increased for all masses but the degree of attenuation was not as drastic as that observed in liquefied sand layers.

CUMULATIVE ENERGY LOSS

Factors that cause attenuation of earthquake motion include drops in stiffness of the ground, as described above, and increases in damping caused by hysteresis. This section discusses the cumulative energy loss index ΔW , which is related to the amount of plastic strain energy absorbed in the ground, and its relationship with the earthquake response characteristics of the ground (Katada et al. 1987, Kazama et al. 1999). Here, cumulative energy loss ΔW is calculated from the area of the stress-strain loop in Figure 5. Sugano and Yanagisawa (1991, 1992) showed that the cumulative energy loss normalized by initial confining pressure, is independent of the element testing procedure. Therefore, in this section, cumulative energy loss ΔW is evaluated as the normalized cumulative energy loss $\Delta W/\sigma_m'$ (hereinafter referred to as the cumulative energy loss), determined by dividing the cumulative energy loss ΔW by the initial mean effective principal stress σ_m' .

Figure 11 shows the depth distribution of cumulative energy loss. In Figure 11(a), which compares the degrees of consolidation, the cumulative energy loss of L4 was larger in clay than in sand, and was the largest in the under-consolidated clay, followed by normally consolidated and over-consolidated clays

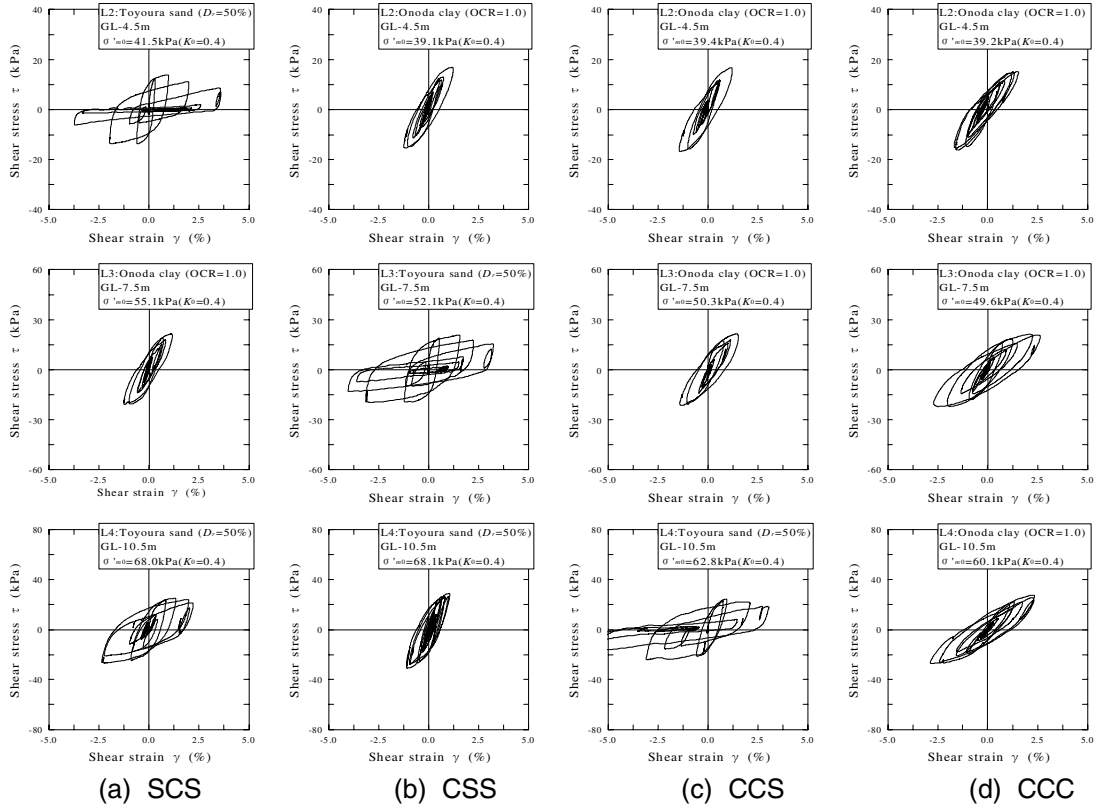
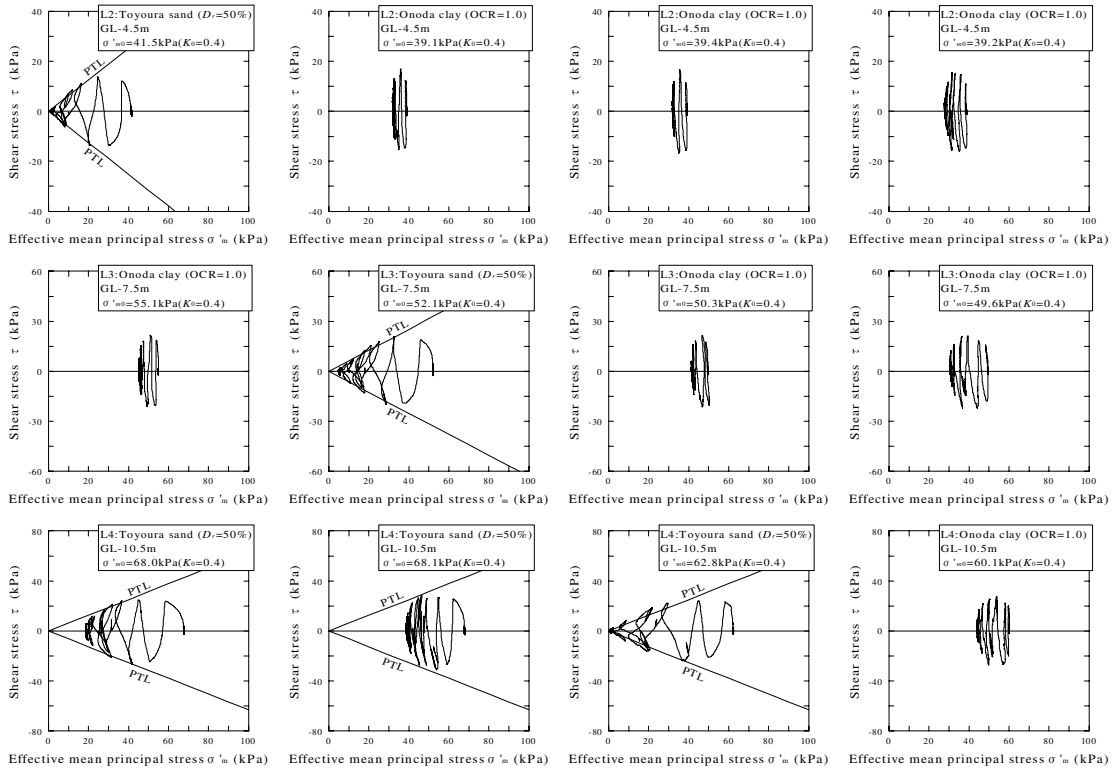
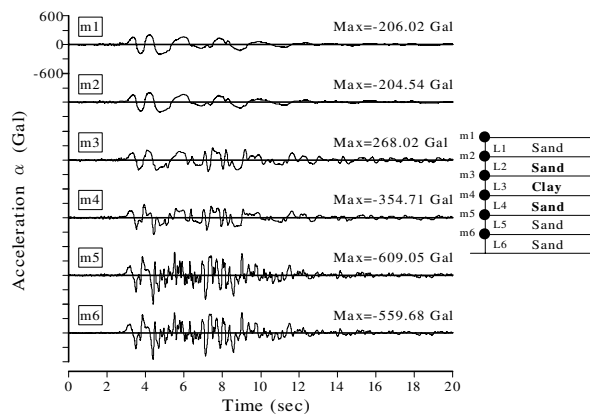


Figure 8 Relationships between shear stress τ and shear strain γ

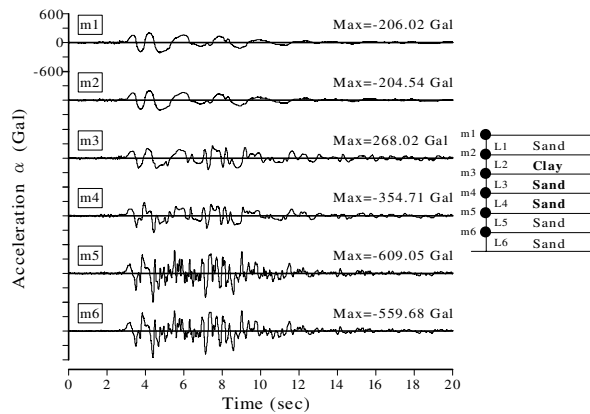


(a) SCS (b) CSS (c) CCS (d) CCC

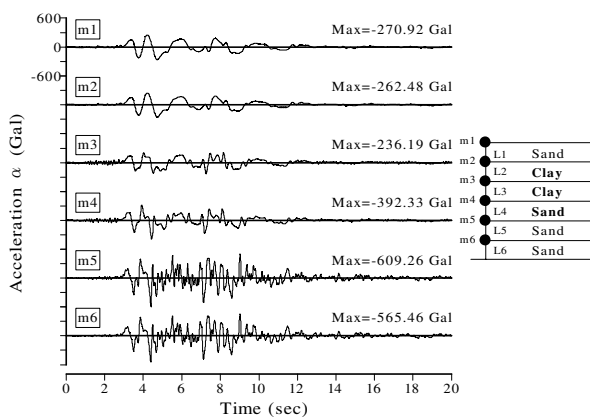
Figure 9 Effective stress paths



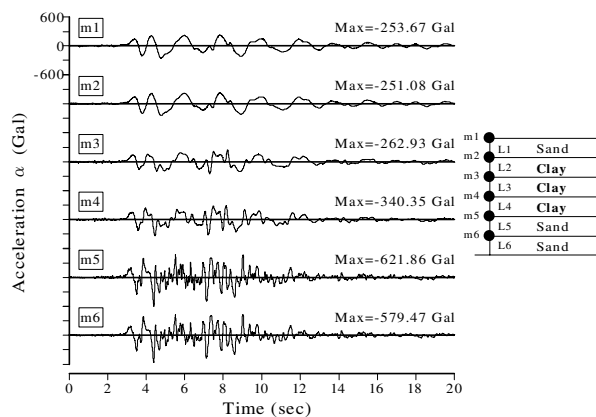
(a) SCS



(b) CSS

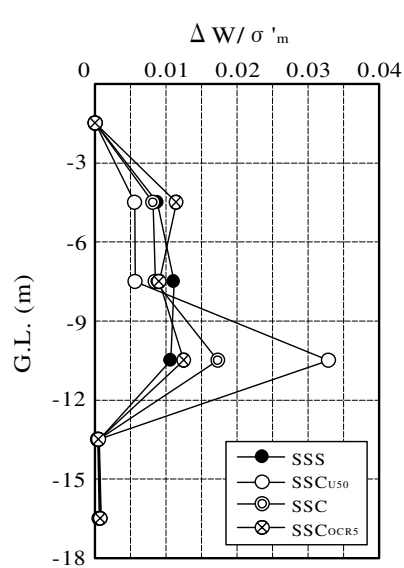


(c) CCS

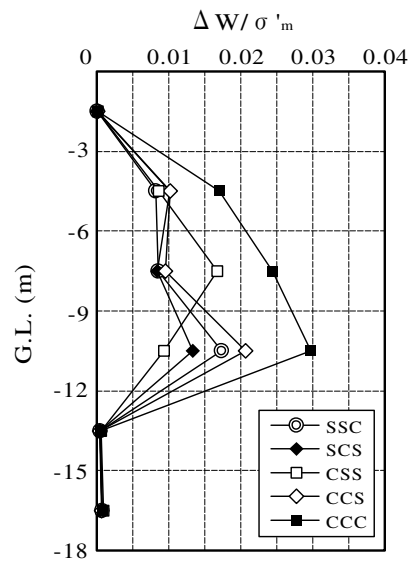


(d) CCC

Figure 10 Acceleration time histories



(a) Comparison of the degree of consolidation and stress history



(b) Comparison of layer order and thickness

Figure 11 Depth distribution of cumulative energy loss

in that order. The larger the cumulative energy loss in L4, the smaller the cumulative energy loss in the upper layers. This was attributable to the large consumption of earthquake energy in L4, which reduced the earthquake motion that was propagated to the upper layers. The result suggests that clay increasingly attenuates earthquake motion as it softens, consuming large amounts of energy and inhibiting the motion's propagation. In Figure 11(b), which compares layer orders and layer thicknesses, the cumulative energy loss was large in sand layers beneath clay layers in SCS, CSS, and CCS. However, in SSC, in which a clay layer underlay sand layers, L2 had a large maximum shear strain but small cumulative energy loss, and their distributions were not similar. This suggests that clay reduces the propagation of earthquake motion but amplifies the long period components, thus increasing the strain in the overlying sand layer, when the sand layer is liquefied and has a reduced natural frequency.

CONCLUSIONS

On-line pseudo-dynamic earthquake response tests have been conducted to analyze the earthquake response characteristics of ground consisting of alternating layers of clay and sand. The study investigated the effects on the earthquake response characteristics of the stress history, degree of consolidation, and configuration of the clay layers. The relationship between cumulative energy loss and ground response characteristics were also analyzed. It was found that:

- (1) The time-history deformation characteristics of clay varied depending on its degree of consolidation and stress history. The difference affected the degree of liquefaction of overlying sand layers, and the strain generated in the overlying layers was the smallest for the under-consolidated clay, followed by normally consolidated clay and over consolidated clay in ascending order.
- (2) Tests in which the depth of a clay layer was changed showed that there was a marked development of strain just beneath the clay layer.
- (3) Cumulative energy loss was larger in clay than in sand, and was largest in the under-consolidated clay, followed by normally consolidated and over-consolidated clays, in that order.

ACKNOWLEDGEMENTS

We thank Mr. Kusakabe of Okumura Corp., who developed the on-line earthquake response tests, for giving us valuable advice in how to progress this study.

REFERENCES

- Akashi N (1972):"Imperial Hotel Verification Research", Pub. Toukoudou, pp.347-359. (In Japanese)
- Alarcon-Guzman, A., Leonards, G.A. & Chameau, J.L. (1988):"Undrained monotonic and cyclic strength of sands", ASCE Journal of Geotechnical Engineering Division, Vol. 114, No. GT10, pp.1089-1109.
- Desai, C. S., Drumm, E. C., and Zaman, M. M. (1985):"Cyclic testing and modeling of interfaces," ASCE, Journal of Geotechnical Engineering, 111(6), pp.793-815.
- Futagawa Y. (1980):"The Imperial Hotel, Tokyo, Japan, pp.1915-1922, F. L. Wright"; GA Global Architecture, No. 53. (In Japanese)
- Fukutake K, (2001):"Base isolation of foundations using ground characteristics", Architectural Institute of Japan, Kanto Region Convention, Structures Group (foundations), Theme: "New Feasible Types of Earthquake Resistant Foundations". (In Japanese)
- JGS (1994):"Earthquake damage due to weak ground motion amplification" Proceedings of Symposium held by the Japanese Geotechnical Society (JGS) Committee on Earthquake Damage due to Weak Ground Motion Amplification. (In Japanese)
- JSCE Earthquake Engineering Committee (1990a):"Reconnaissance Report on the Loma Prieta Earthquake of October 17,1989" JSCE Journal of Construction Management and Engineering, No.421/VI-13, pp.25-42. (in Japanese)
- JSCE Earthquake Engineering Committee(1990b):"Reconnaissance Report on the Loma Prieta Earthquake of October 17,1989" JSCE Journal of Structural Mechanics and Earthquake Engineering, No.422/I-14, pp.11-83. (in Japanese)
- JSCE Earthquake Engineering Committee(1990c):"Reconnaissance Report on the Loma Prieta Earthquake of October 17,1989" JSCE Journal of Geotechnical Engineering, No.424/III-14, pp.19-68. (in Japanese)
- Katada, T., Abe, K. and Higashiyama, A. (1987):"A store of Strain Energy in Liquefaction Process of Saturated Sand", JSCE Journal of Geotechnical Engineering, No.388/III-8, pp.43-50. (In Japanese)
- Kazama, M., Suzuki, T. and Yanagisawa, E. (1999):"Evaluation of Dissipation Energy Accumulated in Surface Ground and Its Application to Liquefaction Prediction", JSCE Journal of Geotechnical Engineering, No.631/III-48, pp.161-177. (In Japanese)
- Kusakabe, S., Morio, S and Arimoto, K. (1990):"Liquefaction Phenomenon of Sand Layers by Using On-Line Computer Test Control Method", Soils and Foundations, Journal of the Japanese Society of Soil Mechanics and Foundation Engineering, Vol.30, No.3, pp.174-184.
- Kusakabe, S., Morio, S., Okabayashi, T., Fujii, T. and Hyodo, M (1999):"Development of a simple shear apparatus and its application to various liquefaction tests", JSCE, Journal of Geotechnical Engineering, No.617/III-46, pp.299-304. (In Japanese)
- Mendoza, M.J. and Auvinet, G (1988):"The Mexico Earthquake of September 19,1985:behavior of building foundations in Mexico City", Earthquake Spectra Journal, EERI, Vol.4, No.4, pp.835-853.
- Shibata A. (1981):"Recent structural analyses for earthquake resistance", Pub. Morikita Shuppan Co.
- Sugano, T. and Yanagisawa, E. (1991):"Undrained shear behavior of sand under surface wave stress conditions", Proceedings of the 9th.Asian Regional Conference on Soil Mechanics and Foundation Engineering, Bangkok, Thailand, Vol.1, pp.71-74.
- Sugano, T. and Yanagisawa, E.(1992):"Cyclic undrained shear behavior of sand under surface wave stress conditions", Proceedings of the 10th.World Conference on Earthquake Engineering, Madrid, Vol.3, pp.1323-1327.
- Yasuhara, K. (1999):"Behavior of a fine-grained soil during the Loma Prieta earthquake" Discussion, Canadian Geotechnical Journal, Vol.36, No.3, pp.582-583.